



Cite this: *Chem. Sci.*, 2023, 14, 3493

All publication charges for this article have been paid for by the Royal Society of Chemistry

Received 8th November 2022
Accepted 27th February 2023

DOI: 10.1039/d2sc06152j

rsc.li/chemical-science

Copper-catalyzed enantioselective diyne cyclization via C(sp²)-O bond cleavage†

Ji-Jia Zhou,^{‡a} Ya-Nan Meng,^{‡a} Li-Gao Liu,^a Yi-Xi Liu,^a Zhou Xu,^{ID} *^b Xin Lu,^{ID} *^a Bo Zhou^a and Long-Wu Ye^{ID} *^{ac}

The functionalization of etheric C–O bonds via C–O bond cleavage is an attractive strategy for the construction of C–C and C–X bonds in organic synthesis. However, these reactions mainly involve C(sp³)-O bond cleavage, and a catalyst-controlled highly enantioselective version is extremely challenging. Here, we report a copper-catalyzed asymmetric cascade cyclization via C(sp²)-O bond cleavage, allowing the divergent and atom-economic synthesis of a range of chromeno[3,4-c]pyrroles bearing a triaryl oxa-quaternary carbon stereocenter in high yields and enantioselectivities. Importantly, this protocol not only represents the first [1,2]-Stevens-type rearrangement via C(sp²)-O bond cleavage, but also constitutes the first example of [1,2]-aryl migration reactions via vinyl cations.

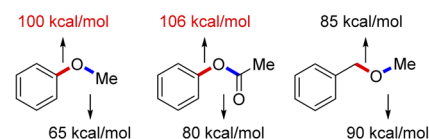
Introduction

The functionalization of etheric C–O bonds via C–O bond cleavage is an attractive strategy for the construction of C–C and C–X bonds in organic synthesis as ethers are stable and readily available building blocks.¹ Nevertheless, the functionalization of an etheric C–O bond is extremely challenging because of its high bond dissociation energy (BDE, 100–110 kcal mol^{−1}, Scheme 1a).² Currently, reactions involving C–O bond cleavage of ethers mainly focus on C–O bond activation and formal C–O bond insertion.^{1,3} The C–O bond activation of ethers, first realized in 1979 by E. Wenkert,⁴ has been demonstrated to be an effective approach for ether bond functionalization via transition metal (Ni, Pd, Ru, Fe, Cr, and Rh) catalysis,^{1,5} but no direct catalytic asymmetric activation of aromatic C–O bonds has been reported to the best of our knowledge.⁶ Formal C–O bond insertions, mainly involving [1,2]-Stevens-type rearrangement reactions of oxonium ylides, have received extensive attention in the past few decades. However, these reactions generally involve the migration of the benzyl and allyl groups via C(sp³)-O bond cleavage,^{3,7} and such a catalyst-controlled highly enantioselective rearrangement is also highly

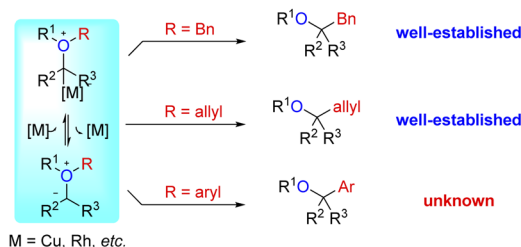
challenging.⁸ Importantly, the related aryl migration reaction via C(sp²)-O bond cleavage has not been explored yet (Scheme 1b).

Vinyl cations have proven to be versatile intermediates in organic synthesis and have attracted particular attention over the past decade due to their unique carbene-like reactivity.⁹

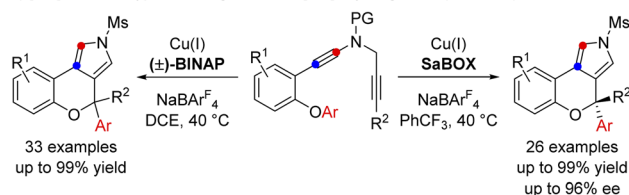
a) Bond dissociation energy (BDE) values of C–O bonds



b) 1,2-Stevens-type rearrangement



c) [1,2]-Stevens-type rearrangement via [1,2]-aryl migration (this work)



♦ 1st [1,2]-Stevens-type rearrangement via [1,2]-aryl migration ♦ high enantioselectivity
♦ practical and atom-economical synthesis ♦ valuable chiral tricyclic N-heterocycles

Scheme 1 Functionalization of etheric C–O bonds involving [1,2]-Stevens-type rearrangement.

^aState Key Laboratory of Physical Chemistry of Solid Surfaces, Key Laboratory of Chemical Biology of Fujian Province, College of Chemistry and Chemical Engineering, Xiamen University, Xiamen 361005, China. E-mail: longwu.ye@xmu.edu.cn; xinlu@xmu.edu.cn; xuzhou@xzhmu.edu.cn

^bJiangsu Key Laboratory of New Drug Research and Clinical Pharmacy, School of Pharmacy, Xuzhou Medical University, Xuzhou 221004, China

^cState Key Laboratory of Organometallic Chemistry, Shanghai Institute of Organic Chemistry, Chinese Academy of Sciences, Shanghai 200032, China

† Electronic supplementary information (ESI) available. CCDC 2192857. For ESI and crystallographic data in CIF or other electronic format see DOI: <https://doi.org/10.1039/d2sc06152j>

‡ J.-J. Z. and Y.-N. M. contributed equally.

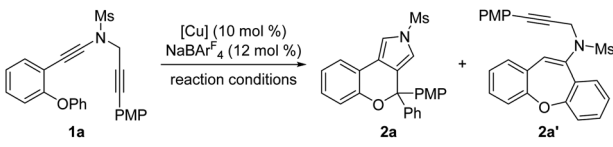


However, successful examples of asymmetric catalysis based on vinyl cation intermediates have been scarcely reported. Very recently, we have developed a facile copper-catalyzed diyne cyclization for the generation of vinyl cations,^{10,11} and achieved a series of asymmetric reactions by this strategy *via* a remote control of enantioselectivity, including intramolecular aromatic C(sp²)-H functionalization,^{10c} vinylic C(sp²)-H functionalization,^{10c} cyclopropanation,^{10e} [1,2]-Stevens-type rearrangement^{10b} and intermolecular annulations with styrenes^{10d} and ketones.^{10a} Inspired by the above results and by our recent study on developing ynamide chemistry for heterocycle synthesis,^{12,13} we envisioned that replacing the benzyl group with an aryl group may lead to C(sp²)-O bond cleavage by employing this asymmetric copper catalysis. Herein, we describe the realization of such a copper-catalyzed enantioselective cascade cyclization *via* C(sp²)-O bond cleavage, allowing the divergent and atom-economic synthesis of various chromeno[3,4-*c*]pyrroles bearing a triaryl oxa-quaternary carbon stereocenter in generally moderate to excellent yields with high enantioselectivities (Scheme 1c). Of note, structural motifs containing a triaryl oxa-quaternary carbon are widely present in natural products and drug molecules.¹⁴ To the best of our knowledge, this protocol not only represents the first [1,2]-Stevens-type rearrangement *via* C(sp²)-O bond cleavage, but also constitutes the first example of [1,2]-aryl migration reactions *via* vinyl cations.

Results and discussion

We started our investigations by using OPh-substituted *N*-propargyl ynamide **1a** as the model substrate, and selected results are listed in Table 1. To our delight, the desired chromeno[3,4-*c*]pyrrole **2a** bearing an oxo-quaternary carbon stereocenter could be obtained in 62% yield in the presence of Cu(CH₃CN)₄PF₆ (10 mol%) as the catalyst according to our designed [1,2]-aryl migration, albeit together with a significant amount of seven-membered product **2a'** *via* a Cu-catalyzed 7-*endo*-dig cyclization (Table 1, entry 1). Further studies revealed that the use of NaBAR^F₄ (12 mol%)¹⁵ as the additive completely prohibited the formation of byproduct **2a'**, and the expected **2a** was delivered in 87% yield (Table 1, entry 2). Of note, NaBAR^F₄ has been widely used as an additive in transition-metal catalysis to enhance the acidity and/or solubility of metal catalysts, thus leading to significantly improved reactivity and selectivity.^{10d} Next, various typical solvents including DCM, toluene, PhCF₃, Et₂O and THF were screened, but failed to give better results (Table 1, entries 3–7). Subsequently, several copper catalysts were also evaluated, and it was found that the use of Cu(CH₃CN)₄BF₄, CuOTf or CuBr as the catalyst led to a slightly decreased yield (Table 1, entries 8, 9, and 11), whereas CuI could not catalyze this cascade cyclization (Table 1, entry 12). When Cu(OTf)₂ was used as the catalyst, **2a'** was obtained as the main product in 40% yield (Table 1, entry 10). Gratifyingly, the desired **2a** could be formed in nearly quantitative yield by employing 12 mol% (±)-BINAP as the ligand (Table 1, entry 13). Finally, decreasing the reaction temperature to 30 °C or 20 °C led to slightly decreased yields (Table 1, entries 14 and 15). Notably, no background benzofuran formation was observed *via* a direct 5-*endo*-dig cyclization in all cases under these Cu-catalyzed conditions.

Table 1 Optimization of reaction conditions for copper-catalyzed cyclization of ynamide **1a**^a



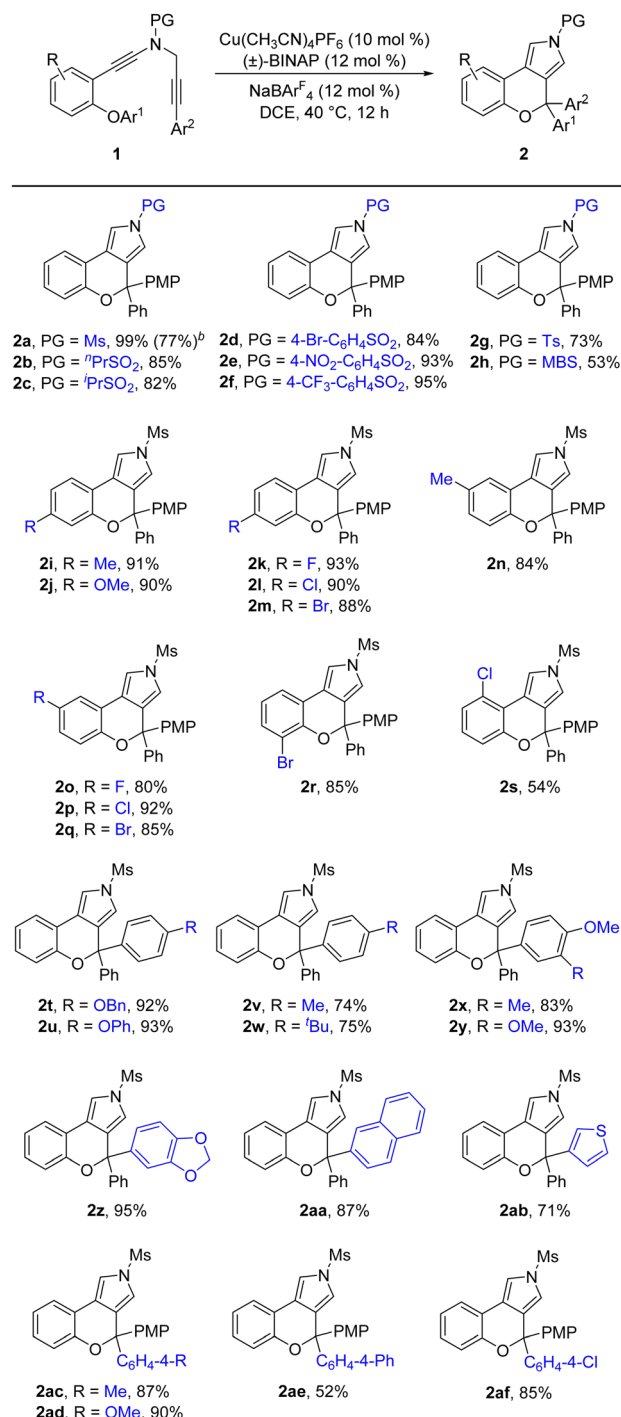
| Entry | [Cu] | Reaction conditions | Yield ^b (%) |
|-----------------|---|--------------------------------|------------------------|
| 1 ^c | Cu(CH ₃ CN) ₄ PF ₆ | DCE, 40 °C, 2 h | 62(15 ^d) |
| 2 | Cu(CH ₃ CN) ₄ PF ₆ | DCE, 40 °C, 2 h | 87 |
| 3 | Cu(CH ₃ CN) ₄ PF ₆ | DCM, 40 °C, 2 h | 86 |
| 4 | Cu(CH ₃ CN) ₄ PF ₆ | Toluene, 40 °C, 2 h | 72 |
| 5 | Cu(CH ₃ CN) ₄ PF ₆ | PhCF ₃ , 40 °C, 2 h | 78 |
| 6 | Cu(CH ₃ CN) ₄ PF ₆ | Et ₂ O, 40 °C, 2 h | <10 |
| 7 | Cu(CH ₃ CN) ₄ PF ₆ | THF, 40 °C, 2 h | <10 |
| 8 | Cu(CH ₃ CN) ₄ BF ₄ | DCE, 40 °C, 2 h | 86 |
| 9 | CuOTf | DCE, 40 °C, 2 h | 81 |
| 10 | Cu(OTf) ₂ | DCE, 40 °C, 2 h | 32(40 ^d) |
| 11 | CuBr | DCE, 40 °C, 2 h | 85 |
| 12 | CuI | DCE, 40 °C, 2 h | <10 |
| 13 ^e | Cu(CH ₃ CN) ₄ PF ₆ | DCE, 40 °C, 2 h | 99 |
| 14 ^e | Cu(CH ₃ CN) ₄ PF ₆ | DCE, 30 °C, 12 h | 90 |
| 15 ^e | Cu(CH ₃ CN) ₄ PF ₆ | DCE, 20 °C, 40 h | 84 |

^a Reaction conditions: **1a** (0.05 mmol), [Cu] (0.005 mmol), NaBAR^F₄ (0.006 mmol), solvent (1 mL), 20–40 °C, 2–40 h, in vials. ^b Measured by ¹H NMR using 1,3,5-trimethoxybenzene as the internal standard. ^c Without NaBAR^F₄. ^d Yield of **2a'**. ^e With (±)-BINAP (0.006 mmol). Ms = methanesulfonyl, PMP = 4-methoxyphenyl, NaBAR^F₄ = sodium tetrakis[3,5-bis(trifluoromethyl)phenyl]borate, DCE = 1,2-dichloroethane.

Having established the optimal reaction conditions (Table 1, entry 13), we next sought to explore the scope of this cascade reaction. As shown in Table 2, we initially investigated the scope of different *N*-protecting groups of the *N*-propargyl ynamides. Apart from the Ms-protected ynamide, the reaction proceeded smoothly with other alkyl sulfonyl groups, providing the corresponding chromeno[3,4-*c*]pyrroles **2b** and **2c** bearing an oxo-quaternary carbon stereocenter in 82–85% yields. Then, diynes with a diverse array of aryl sulfonyl groups, such as Bs (4-bromobenzenesulfonyl), Ts, and MBS were suitable substrates for this cascade cyclization, affording the desired products **2d–2h** in generally good to excellent yields. The role of the electronic properties of the aromatic ring was next studied, and it was found that substitutions including both electron-donating and -withdrawing groups on the aromatic ring occurred efficiently, delivering the corresponding products **2i–2m** with yields ranging from 88% to 93%. Substitutions with various electronic properties at the different positions of the phenyl ring had little effect on this protocol, and the expected chromeno[3,4-*c*]pyrroles **2n–2s** were obtained in 54–92% yields. In addition, different aryl-substituted diynes on *N*-propargyl moieties (Ar²) proved to be applicable substrates for this reaction, thus leading to anticipated products **2t–2w** in high yields. Ynamides bearing disubstituents on the aryl ring could participate in this transformation as well to give rise to **2x–2z** in 83–95% yields. Furthermore, the reaction was also extended to naphthyl- and thienyl-substituted diynes,



Table 2 Reaction scope for the formation of chromeno[3,4-*c*]pyrroles **2**^a



^a Reaction conditions: **1** (0.1 mmol), Cu(CH₃CN)₄PF₆ (0.01 mmol), NaBARF₄ (0.012 mmol), (±)-BINAP (0.012 mmol), DCE (2 mL), 40 °C, 12 h, in vials; yields are for the isolated products. ^b Formed from ynamide substrate **1ag**. Ts = *p*-toluenesulfonyl. MBS = 4-methoxybenzenesulfonyl.

enabling an approach to the expected products **2aa** in 87% yield and **2ab** in 71% yield, respectively. Finally, we examined the effect of the migratory aryl groups, and found that the reaction of 4-Me,

4-OMe, 4-Ph and 4-Cl substituted diynes was also well compatible with the established conditions, thus providing the desired chromeno[3,4-*c*]pyrroles **2ac–2af** in 52–90% yields. Of note, the synthesis of product **2a** could also be achieved in 77% yield from ynamide substrate **1ag**.¹⁵ Attempts to extend the reaction to ynamide **1ah** bearing a substituent at the *ortho* position of the aryl group of Ar² and ynamide **1ai** with an alkyl group only gave a complex mixture of products.¹⁵

After accomplishing the above copper-catalyzed cascade cyclization/[1,2]-aryl migration reaction of *N*-propargyl ynamides, we attempted to establish the catalytic asymmetric version of this reaction (for more details see ESI Tables 1 and 2).[†] As summarized in Table 3, we were pleased to find that the expected chiral chromeno[3,4-*c*]pyrrole (+)-**2a** bearing a oxo-quaternary carbon stereocenter could be furnished in 75% yield with 75% ee by the use of phenyl-substituted BOX (bisoxazoline) ligand **L1** (Table 3, entry 1). Encouraged by this preliminary result, we next investigated assorted types of chiral BOX ligands. However, employing several typical chiral BOX ligands **L2–L6** led to diminished yields and enantioselectivities (Table 3, entries 2–6). In view of the fact that BOX ligands could be readily modified with the side-arm strategy established by Tang's group,¹⁶ we attempted to alter the dibenzyl group of the BOX ligand. Gratifyingly, the enantioselectivity was significantly improved by employing 3,5-diethoxyl benzyl-substituted BOX ligand **L14** after a large amount of explorations (Table 3, entries 7–17), and the desired chiral chromeno[3,4-*c*]pyrrole (+)-**2a** was delivered in 82% yield with 92% ee (Table 3, entry 14). Among various typical organic solvents screened for this cascade cyclization (Table 3, entries 18–21), PhCF₃ was found to be optimal, providing the anticipated (+)-**2a** in 92% yield with 94% ee (Table 3, entry 19).

Under the optimized conditions for the asymmetric version of this cascade cyclization (Table 3, entry 19), the substrate scope for synthesis of enantioenriched chromeno[3,4-*c*]pyrroles was then examined. As depicted in Table 4, except for the Ms-protected ynamide **1a**, this enantioselective cyclization is remarkably tolerant of various *N*-protected ynamides, including ^tPrSO₂-, ⁱPrSO₂-, Bs-, 4-NO₂-C₆H₄SO₂-, 4-CF₃-C₆H₄SO₂-, Ts- and MBS-protected *N*-propargyl ynamides, thus affording the corresponding chiral chromeno[3,4-*c*]pyrroles (+)-**2b**–(+)-**2h** in 60–99% yields and 78–94% ees. Furthermore, this asymmetric process readily accommodated substitution at the 3- or 4-position of the phenyl ring with electron-deficient and -rich substituents comprising Me, OMe, F, Cl, and Br, enabling the assembly of the expected enantioenriched chromeno[3,4-*c*]pyrroles (+)-**2i**–(+)-**2n** in generally excellent yields with excellent enantioselectivities. Additionally, switching the PMP-substituent of diyne to other electron-rich substituents such as OBn-, OPh-, Me-, and ^tBu-substituted diynes led to the asymmetric rearrangement process to furnish the desired products (+)-**2t**–(+)-**2w** in high yields and enantiopurities. Of note, the reaction time was considerably prolonged on decreasing the electronic density of the phenyl groups, such as Me- and ^tBu-substituted ynamides **1v** and **1w**, which is similar to our previous reports.¹⁰ What's more, diynes bearing different disubstituents on the phenyl ring were accommodated to provide the expected products (+)-**2x**–(+)-**2z** in 95–99% yields and 93–96% ees.



Table 3 Optimization of reaction conditions for asymmetric copper-catalyzed cyclization of ynamide **1a**^a

Reaction scheme for Table 3: Ynamide **1a** reacts with $\text{Cu}(\text{CH}_3\text{CN})_4\text{PF}_6$ (10 mol %), **L** (12 mol %), and NaBARF_4 (12 mol %) under reaction conditions to form product **(+)-2a**.

Chemical structures of ligands **L1** through **L17** are shown below the reaction scheme.

| Entry | L | Reaction conditions | Yield ^b (%) | ee ^c (%) |
|-------|------------|-------------------------------|------------------------|---------------------|
| 1 | L1 | DCE, 40 °C, 12 h | 75 | 75 (+) |
| 2 | L2 | DCE, 40 °C, 18 h | <10 | — |
| 3 | L3 | DCE, 40 °C, 24 h | 42 | 10 (+) |
| 4 | L4 | DCE, 40 °C, 12 h | 71 | 58 (+) |
| 5 | L5 | DCE, 40 °C, 12 h | 74 | 74 (+) |
| 6 | L6 | DCE, 40 °C, 12 h | 72 | 69 (+) |
| 7 | L7 | DCE, 40 °C, 12 h | 74 | 75 (+) |
| 8 | L8 | DCE, 40 °C, 12 h | 73 | 72 (+) |
| 9 | L9 | DCE, 40 °C, 12 h | 71 | 72 (+) |
| 10 | L10 | DCE, 40 °C, 12 h | 71 | 70 (+) |
| 11 | L11 | DCE, 40 °C, 18 h | 72 | 58 (+) |
| 12 | L12 | DCE, 40 °C, 12 h | 75 | 77 (+) |
| 13 | L13 | DCE, 40 °C, 12 h | 80 | 91 (+) |
| 14 | L14 | DCE, 40 °C, 12 h | 82 | 92 (+) |
| 15 | L15 | DCE, 40 °C, 16 h | 80 | 92 (+) |
| 16 | L16 | DCE, 40 °C, 16 h | 79 | 92 (+) |
| 17 | L17 | DCE, 40 °C, 30 h | 65 | <10 (+) |
| 18 | L14 | Toluene, 40 °C, 10 h | 82 | 93 (+) |
| 19 | L14 | PhCF_3 , 40 °C, 12 h | 92 | 94 (+) |
| 20 | L14 | PhF , 40 °C, 10 h | 85 | 92 (+) |
| 21 | L14 | PhCl , 40 °C, 10 h | 84 | 92 (+) |

^a Reaction conditions: **1a** (0.05 mmol), $\text{Cu}(\text{CH}_3\text{CN})_4\text{PF}_6$ (0.005 mmol), **L** (0.006 mmol), NaBARF_4 (0.006 mmol), solvent (1 mL), in vials.
^b Measured by ¹H NMR using 1,3,5-trimethoxybenzene as the internal standard.
^c Determined by HPLC analysis.

Chemical structures of ligands **L7** through **L17** are shown below the reaction scheme:

- L7**, R = 4- CF_3
- L8**, R = 4-OMe
- L9**, R = 4- Pr
- L10**, R = 4- tBu
- L11**, R = 4-Ph
- L12**, R = 3,5- Me_2
- L13**, R = 3,5-(OMe)₂
- L14**, R = 3,5-(OEt)₂
- L15**, R = 3,5-(O^iPr)₂
- L16**, R = 3,5-(O^iPr)₂
- L17**, R = 3,5-(OBn)₂

^a Reaction conditions: **1a** (0.05 mmol), $\text{Cu}(\text{CH}_3\text{CN})_4\text{PF}_6$ (0.005 mmol), **L** (0.006 mmol), NaBARF_4 (0.006 mmol), solvent (1 mL), in vials.
^b Measured by ¹H NMR using 1,3,5-trimethoxybenzene as the internal standard.
^c Determined by HPLC analysis.

Next, naphthyl- and thienyl-substituted *N*-propargyl ynamides performed well in this asymmetric tandem reaction, and the corresponding products **(+)-2aa** and **(+)-2ab** were isolated in 86% yield with 93% ee and 93% yield with 95% ee, respectively. Further modifications on the substituents of the migratory aryl group such as 4-Me, 4-Ph and 4-Cl substituents were also accomplished to furnish the desired products **(+)-2ac**, **(+)-2ae** and **(+)-2af** in excellent yields with remarkably high enantioselectivities. Finally, the reaction occurred smoothly by employing a chiral catalyst with the opposite configuration, and delivered the desired **(-)-2a** with the

Table 4 Reaction scope for the formation of chiral chromeno[3,4-c]pyrroles **(+)-2**^a

Reaction scheme for Table 4: Ynamide **1** reacts with $\text{Cu}(\text{CH}_3\text{CN})_4\text{PF}_6$ (10 mol %), **L14** (12 mol %), and NaBARF_4 (12 mol %) in PhCF_3 at 40 °C for 12 h to form product **(+)-2**.

Chemical structures of products **(+)-2a** through **(-)-2a** are shown below the reaction scheme.

Reaction conditions for **(+)-2a** through **(-)-2a** are shown below the reaction scheme:

- (+)-2a**, PG = Ms, 94%, 94% ee
- (+)-2b**, PG = PrSO_2 , 84%, 86% ee
- (+)-2c**, PG = PrSO_2 , 77%, 85% ee
- (+)-2d**, PG = 4-Br- $\text{C}_6\text{H}_4\text{SO}_2$, 85%, 88% ee
- (+)-2e**, PG = 4- NO_2 - $\text{C}_6\text{H}_4\text{SO}_2$, 96%, 85% ee
- (+)-2f**, PG = 4- CF_3 - $\text{C}_6\text{H}_4\text{SO}_2$, 99%, 86% ee
- (+)-2g**, PG = Ts, 69%, 78% ee
- (+)-2h**, PG = MBS, 60%, 79% ee
- (+)-2i**, R = Me, 91%, 91% ee
- (+)-2j**, R = OMe, 91%, 91% ee
- (+)-2k**, R = F, 99%, 91% ee
- (+)-2l**, R = Cl, 92%, 90% ee
- (+)-2m**, 92%, 85% ee
- (+)-2n**, 80%, 80% ee
- (+)-2o**, 94%, 95% ee
- (+)-2p**, 94%, 94% ee
- (+)-2q**, 83%, 94% ee (2 d)
- (+)-2r**, 92%, 94% ee (4 d)
- (+)-2s**, 96%, 93% ee
- (+)-2t**, 95%, 94% ee
- (+)-2u**, 99%, 96% ee
- (+)-2aa**, 86%, 93% ee (4 d)
- (+)-2ab**, 93%, 95% ee (4 d)
- (+)-2ac**, 96%, 95% ee
- (+)-2ae**, 95%, 93% ee (4 d)
- (+)-2af**, 99%, 93% ee
- (-)-2a**, 96%, 94% ee

^a Reaction conditions: **1** (0.1 mmol), $\text{Cu}(\text{CH}_3\text{CN})_4\text{PF}_6$ (0.01 mmol), NaBARF_4 (0.012 mmol), **L14** (0.012 mmol), PhCF_3 (2 mL), 40 °C, 12–96 h, in vials; yields are for the isolated products; ees are determined by HPLC analysis. ^b (**R**)-**L14** instead of **L14**.

opposite configuration in 96% yield with 94% ee. The absolute configuration of **(+)-2a** was confirmed by X-ray diffraction analysis (Fig. 1)¹⁷

Gram-scale reactions and further synthetic applications of the as-synthesized tricyclic heterocycles were then explored



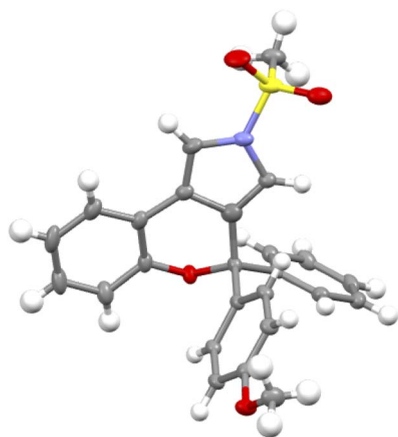
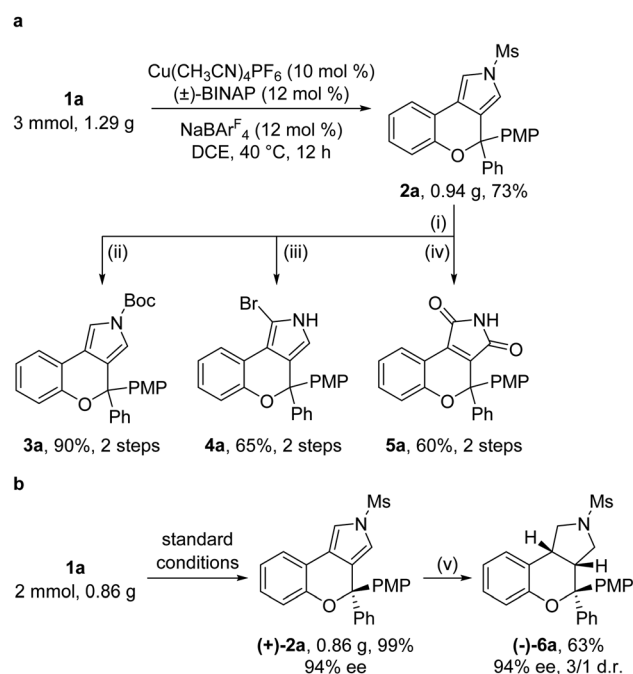


Fig. 1 Structure of compound (+)-2a in its crystal form.

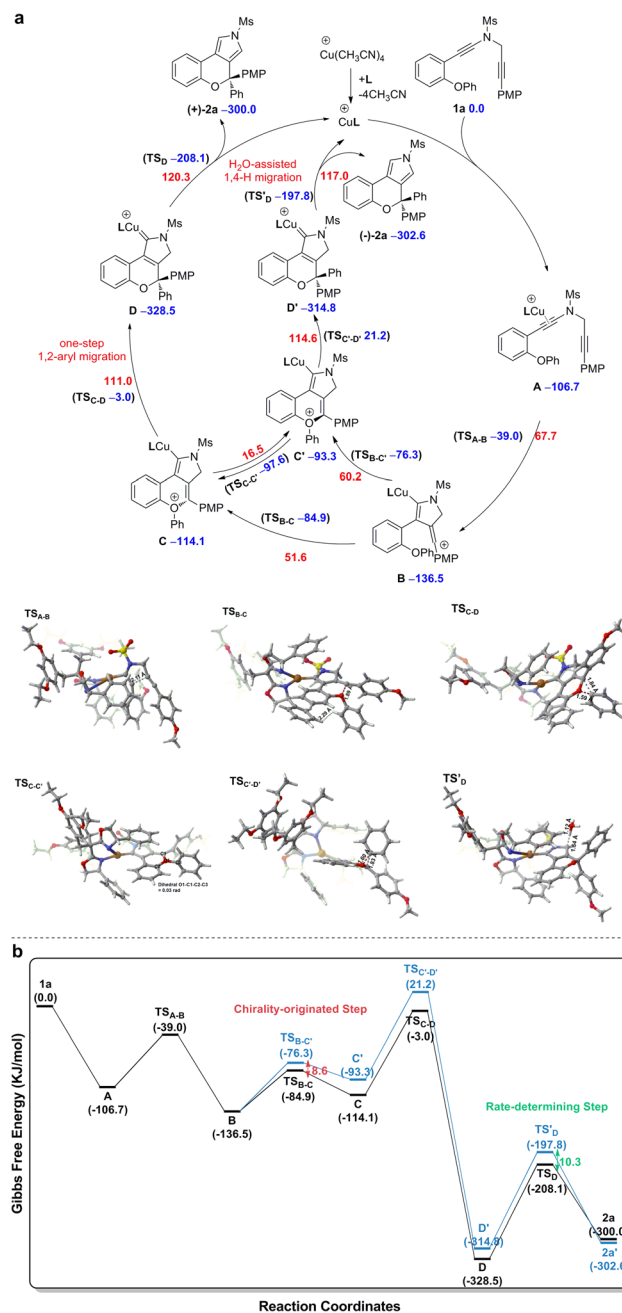
(Scheme 2). First, the Ms protecting group in chromeno[3,4-*c*]pyrrole **2a**, which could be synthesized on the gram scale in 73% yield under standard conditions, was readily removed by treatment with KOH, followed by protection with the Boc group, site-selective bromination by NBS (*N*-bromosuccinimide) and oxidation by the UHP (urea-hydrogen peroxide complex) to lead to the corresponding products **3a** (90%, 2 steps), **4a** (65%, 2 steps) and **5a** (60%, 2 steps), respectively (Scheme 2a). Moreover, the asymmetric cyclization reaction of **1a** on the gram scale under standard conditions was also performed, and the

desired (+)-**2a** was formed in 99% yield and 94% ee, which could be reduced into the pyrrolidine-fused product (–)-**6a** containing three contiguous stereocenters in 63% yield with 94% ee and 3 : 1 dr (Scheme 2b).

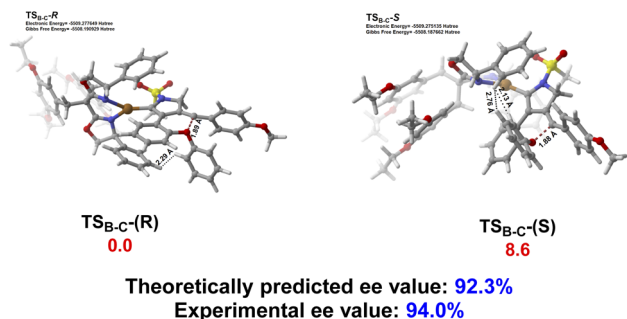
Based on the above experimental observations, our previously published results¹⁰ and present density functional theory



Scheme 2 Scale-up reaction and product elaboration. Reagents and conditions: (i) KOH (5 equiv.), THF : MeOH/1 : 1, 50 °C, 2 h. (ii) 4-DMAP (20 mol%), (Boc)₂O (3 equiv.), Et₃N (4 equiv.), DCM, rt, 2 h. (iii) NBS (1.05 equiv.), THF, –78 °C, 1 h. (iv) UHP (5 equiv.), HFIP (hexafluoroisopropanol), 45 °C, 24 h. (v) H₂ (7 Mpa), Pd/C (20 mol%), EtOH : AcOH/10 : 1, 100 °C, 3.5 h.



Scheme 3 (a) Mechanism for the synthesis of chromeno[3,4-*c*]pyrrole (+)-**2a** from diyne substrate **1a**. (b) Free energy profile for the synthesis of chromeno[3,4-*c*]pyrrole (+)-**2a** from diyne substrate **1a**. Relative free energies (ΔG , in kJ mol^{–1}) of all the transition states and intermediates were computed at the SMD(PhCF₃)-M06/6-31G(d,p) & LANL2DZ level of theory, with the electronic energy of all the transition states and intermediates recomputed at the SMD(PhCF₃)-M06-D3/def2-TZVPP level of theory. Color code: red = O; white = H; gray = C; yellow = S; blue = N; brown = Cu.



Scheme 4 The geometries and relative free energies (ΔG , in kJ mol^{-1}) of the transition state $[\text{CuL14}]$ -R TS_{B-C} and $[\text{CuL14}]$ -S TS_{B-C} with the chiral ligand. Relative free energies (ΔG , in kJ mol^{-1}) of all the transition states and intermediates were computed at the SMD(PhCF₃)-M06/6-31G(d,p)&LANL2DZ level of theory, with the electronic energy of all the transition states and intermediates recomputed at the SMD(PhCF₃)-M06-D3/def2-TZVPP level of theory. Color code: red = O; white = H; gray = C; yellow = S; blue = N; brown = Cu.

(DFT) calculations (for more details see the ESI†), a plausible mechanism involving vinyl cation intermediates¹¹ for the formation of chiral chromeno[3,4-*c*]pyrrole (+)-**2a** from diyne **1a** is displayed in Scheme 3. The Cu^I catalyst first preferentially coordinates to the electron-rich amide-tethered C≡C bond of **1a** to form precursor **A**, followed by intramolecular trapping by the *N*-propargyl moiety, affording the vinyl cation intermediate **B**. Subsequent intramolecular trapping of intermediate **B** by the phenoxy group leads to the chiral oxonium intermediate **C** with a free energy barrier of 51.6 kJ mol^{-1} . Next, a [1,2]-Stevens-type rearrangement within the oxonium cation **C** affords the copper carbene intermediate **D** via a stereospecific one-step [1,2]-aryl migration pathway with a free energy barrier of 111.0 kJ mol^{-1} . Finally, the same as our previous findings,¹⁰ a formal [1,4]-H migration assisted by trace H₂O in the reaction system via two consecutive steps of proton transfer and demetallation occurs to deliver the final chiral product (+)-**2a**, with a free energy barrier of 120.3 kJ mol^{-1} . As alluded above, the reaction can smoothly occur under the experimental conditions, with the H₂O-assisted 1,4-H migration being the rate-determining step.

The origin of enantioselective synthesis of chiral (+)-**2a** is also theoretically unraveled with the chiral **L14** ligated to the Cu^I center in the process of intramolecular trapping of the vinyl cation by the phenoxy group (**B** → **C**), as the O atom orientation of the phenoxy group separates the configuration of the final chiral product in the process of intramolecular cyclization. More importantly, the difference in barrier heights of the subsequent rate-determining step, *i.e.* the H₂O-assisted 1,4-H migration process helps maintain the enantioselectivity in a kinetic control manner, although it is unraveled by DFT computations that the chiral oxonium cation generated in the aforementioned chirality-originated step easily undergoes an inversion in the reaction.

The free energy of the transition state $[\text{CuL14}]$ -R TS_{B-C} is predicted to be 8.6 kJ mol^{-1} lower than that of $[\text{CuL14}]$ -S TS_{B-C}, which is well in line with the experimental ee value of 94%. Also, the difference in free energies (10.3 kJ mol^{-1}) of the two

transition states in the rate-determining step, *i.e.* the H₂O-assisted H-migration process (TS_B and TS'_B) again supports the experimental ee value of 94%, which shows that there is no loss of enantioselectivity in the process from **C** to **2a** attributed to the kinetic control of the subsequent rate-determining step as well. Further observation on their stereogenic configurations indicates that the steric repulsion between the bulky chiral ligand **L14** and the branched groups in the substrate is critical to the generation of enantioselectivity in a remote control manner (Scheme 4).

Conclusions

In summary, we have developed a copper-catalyzed asymmetric cascade cyclization via C(sp²)-O bond cleavage, which not only represents the first [1,2]-Stevens-type rearrangement via C(sp²)-O bond cleavage, but also constitutes the first example of [1,2]-aryl migration reactions via vinyl cations. This method enables the divergent, practical and atom-economic synthesis of a range of chromeno[3,4-*c*]pyrroles bearing a triaryl oxa-quaternary carbon stereocenter in high yields and enantioselectivities (up to 96% ee) under mild conditions. Moreover, theoretical calculations provide further evidence for this vinyl cation involved cyclization/rearrangement and the origin of enantioselectivity. We envision that the above findings will open up new horizons in the field of catalytic asymmetric reactions based on etheric C-O bond functionalization, [1,2]-Stevens-type rearrangement and vinyl cations.

Data availability

Data for the crystal structures reported in this paper have been deposited at the Cambridge Crystallographic Data Centre (CCDC) under the deposition numbers CCDC 2192857 ((+)-**2a**). All other data supporting the findings of this study, including experimental procedures and compound characterization, are available within the paper and its ESI files, or from the corresponding authors on request.†

Author contributions

J.-J. Z., Y.-N. M., Y.-X. L., Z. X., and B. Z. performed the experiments. L.-G. L. and X. L. performed the DFT calculations. L.-W. Y. conceived and directed the project and wrote the paper. All authors discussed the results and commented on the manuscript.

Conflicts of interest

There are no conflicts to declare.

Acknowledgements

We are grateful for financial support from MOST (2021YFC2100100), the National Natural Science Foundation of China (22125108, 22121001 and 92056104), the Natural Science Foundation of Jiangsu Province (BK20211059), the President Research Funds from Xiamen University (20720210002), and



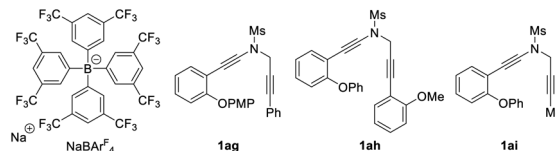
NFFTBS (J1310024). We thank Mr Zanbin Wei from Xiamen University for assistance with X-ray crystallographic analysis.

Notes and references

- For recent selected reviews, see: (a) J. Becica and D. C. Leitch, *Synlett*, 2021, **32**, 641; (b) B. Zhao, T. Rogge, L. Ackermann and Z. Shi, *Chem. Soc. Rev.*, 2021, **50**, 8903; (c) Z. Qiu and C.-J. Li, *Chem. Rev.*, 2020, **120**, 10454; (d) T. B. Boit, A. S. Bulger, J. E. Dander and N. K. Garg, *ACS Catal.*, 2020, **10**, 12109.
- K. Chen, X.-S. Zhang and Z.-J. Shi, *Pure Appl. Chem.*, 2014, **86**, 361.
- For recent selected reviews, see: (a) V. N. Nair and U. K. Tambar, *Org. Biomol. Chem.*, 2022, **20**, 3427; (b) C. Empel, S. Jana and R. M. Koenigs, *Synthesis*, 2021, **53**, 4567; (c) S. Jana, Y. Guo and R. M. Koenigs, *Chem.-Eur. J.*, 2021, **27**, 1270; (d) G. K. Murphy, C. Stewart and F. G. West, *Tetrahedron*, 2013, **69**, 2667; (e) D. M. Hodgson, F. Y. T. M. Pierard and P. A. Stupple, *Chem. Soc. Rev.*, 2001, **30**, 50.
- E. Wenkert, E. L. Michelotti and C. S. Swindell, *J. Am. Chem. Soc.*, 1979, **101**, 2246.
- For selected reviews, see: (a) Y.-Y. Huang, C. Cai, X. Yang, Z.-C. Lv and U. Schneider, *ACS Catal.*, 2016, **6**, 5747; (b) B. Su, Z.-C. Cao and Z.-J. Shi, *Acc. Chem. Res.*, 2015, **48**, 886; (c) D.-G. Yu, B.-J. Li and Z.-J. Shi, *Acc. Chem. Res.*, 2010, **43**, 1486.
- For a recent example on the atroposelective cross-coupling of an inert aromatic C–O bond, see: J. Zhang, T. Sun, Z. Zhang, H. Cao, Z. Bai and Z.-C. Cao, *J. Am. Chem. Soc.*, 2021, **143**, 18380.
- For selected examples, see: (a) V. N. Nair, V. Kojasoy, C. J. Laconsay, W. Y. Kong, D. J. Tantillo and U. K. Tambar, *J. Am. Chem. Soc.*, 2021, **143**, 9016; (b) N. Guranova, D. Dar'in, G. Kantin and M. Krasavin, *Eur. J. Org. Chem.*, 2021, 3411; (c) D. Dar'in, G. Kantin, O. Bakulina, A. Inyutina, E. Chupakhin and M. Krasavin, *J. Org. Chem.*, 2020, **85**, 15586; (d) S. Jana, Z. Yang, C. Pei, X. Xu and R. M. Koenigs, *Chem. Sci.*, 2019, **10**, 10129; (e) J. Zhang, Z. Liao, L. Chen and S. Zhu, *Chem.-Eur. J.*, 2019, **25**, 9405; (f) M. Kitamura, M. Kisanuki, K. Kanemura and T. Okauchi, *Org. Lett.*, 2014, **16**, 1554; (g) D. M. Jaber, R. N. Burgin, M. Helper, P. Y. Zavalij and M. P. Doyle, *Org. Lett.*, 2012, **14**, 1676; (h) D. J. Mack, L. A. Batory and J. T. Njardarson, *Org. Lett.*, 2012, **14**, 378; (i) D. M. Jaber, R. N. Burgin, M. Hepler, P. Zavalij and M. P. Doyle, *Chem. Commun.*, 2011, **47**, 7623; (j) J. Wang, in *Comprehensive Organometallic Chemistry III*, ed. D. M. P. Mingos and R. H. Crabtree, Elsevier, Oxford, 2007, vol. 11, p. 151; (k) G. K. Murphy and F. G. West, *Org. Lett.*, 2006, **8**, 4359; (l) G. K. Murphy and F. G. West, *Org. Lett.*, 2005, **7**, 1801; (m) F. P. Marmsäter, G. K. Murphy and F. G. West, *J. Am. Chem. Soc.*, 2003, **125**, 14724; (n) N. P. Karche, S. M. Jachak and D. D. Dhavale, *J. Org. Chem.*, 2001, **66**, 6323; (o) F. G. West, B. N. Naidu and R. W. Tester, *J. Org. Chem.*, 1994, **59**, 6892; (p) F. G. West, T. H. Eberlein and R. W. Tester, *J. Chem. Soc., Perkin Trans. 1*, 1993, **1**, 2857; (q) T. H. Eberlein, F. G. West and R. W. Tester, *J. Org. Chem.*, 1992, **57**, 3479; (r) E. J. Roskamp and C. R. Johnson, *J. Am. Chem. Soc.*, 1986, **108**, 6062; (s) J. B. Brogan and C. K. Zercher, *Tetrahedron Lett.*, 1998, **39**, 1691; (t) J. B. Brogan, C. K. Zercher, C. B. Bauer and R. D. Rogers, *J. Org. Chem.*, 1997, **62**, 3902; (u) K. Friedrich, U. Jansen and W. Kirmse, *Tetrahedron Lett.*, 1985, **26**, 193; (v) H. Nozaki, H. Takaya and R. Noyori, *Tetrahedron*, 1966, **22**, 3393; (w) C. D. Gutsche and M. Hillman, *J. Am. Chem. Soc.*, 1954, **76**, 2236.
- For recent selected examples, see: (a) M. M.-C. Lo and G. C. Fu, *Tetrahedron*, 2001, **57**, 2621; (b) S. Kitagaki, Y. Yanamoto, H. Tsutsui, M. Anada, M. Nakajima and S. Hashimoto, *Tetrahedron Lett.*, 2001, **42**, 6361; (c) J. S. Clark, M. Fretwell, G. A. Whitlock, C. J. Burns and D. N. A. Fox, *Tetrahedron Lett.*, 1998, **39**, 97; (d) M. P. Doyle, D. G. Ene, D. C. Forbes and J. S. Tedrow, *Tetrahedron Lett.*, 1997, **38**, 4367; (e) K. Ito, M. Yoshitake and T. Katsuki, *Tetrahedron*, 1996, **52**, 3905; (f) H. Nozaki, H. Takaya, S. Moriuti and R. Noyori, *Tetrahedron*, 1968, **24**, 3655.
- For recent reviews, see: (a) X.-J. Liu, Y. Xu, C. Tang, P.-C. Qian and L.-W. Ye, *Sci. China: Chem.*, 2022, **65**, 20; (b) M. Niggemann and S. Gao, *Angew. Chem., Int. Ed.*, 2018, **57**, 16942; for recent selected examples, see: (c) T. Ikeuchi, S. Inuki, S. Oishi and H. Ohno, *Angew. Chem., Int. Ed.*, 2019, **58**, 7792; (d) B. Wigman, S. Popov, A. L. Bagdasarian, B. Shao, T. R. Benton, C. G. Williams, S. P. Fisher, V. Lavallo, K. N. Houk and H. M. Nelson, *J. Am. Chem. Soc.*, 2019, **141**, 9140; (e) S. Popov, B. Shao, A. L. Bagdasarian, T. R. Benton, L. Zou, Z. Yang, K. N. Houk and H. M. Nelson, *Science*, 2018, **361**, 381; (f) S. E. Cleary, M. J. Hensinger and M. Brewer, *Chem. Sci.*, 2017, **8**, 6810.
- For recent selected examples, see: (a) L.-J. Qi, C.-T. Li, Z.-Q. Huang, J.-T. Jiang, X.-Q. Zhu, X. Lu and L.-W. Ye, *Angew. Chem., Int. Ed.*, 2022, **61**, e202210637; (b) F.-L. Hong, C.-Y. Shi, P. Hong, T.-Y. Zhai, X.-Q. Zhu, X. Lu and L.-W. Ye, *Angew. Chem., Int. Ed.*, 2022, **61**, e202115554; (c) X.-Q. Zhu, P. Hong, Y.-X. Zheng, Y.-Y. Zhen, F.-L. Hong, X. Lu and L.-W. Ye, *Chem. Sci.*, 2021, **12**, 9466; (d) F.-L. Hong, Y.-B. Chen, S.-H. Ye, G.-Y. Zhu, X.-Q. Zhu, X. Lu, R.-S. Liu and L.-W. Ye, *J. Am. Chem. Soc.*, 2020, **142**, 7618; (e) F.-L. Hong, Z.-S. Wang, D.-D. Wei, T.-Y. Zhai, G.-C. Deng, X. Lu, R.-S. Liu and L.-W. Ye, *J. Am. Chem. Soc.*, 2019, **141**, 16961.
- For the related gold-catalyzed generation of vinyl cations from diynes, see: (a) A. Ahrens, J. Schwarz, D. M. Lustosa, R. Pourkaveh, M. Hoffmann, F. Rominger, M. Rudolph, A. Dreuw and A. S. K. Hashmi, *Chem.-Eur. J.*, 2020, **26**, 5280; (b) S. Tavakkolifard, K. Sekine, L. Reichert, M. Ebrahimi, K. Museridz, E. Michel, F. Rominger, R. Babaahmadi, A. Ariafard, B. F. Yates, M. Rudolph and A. S. K. Hashmi, *Chem.-Eur. J.*, 2019, **25**, 12180; (c) T. Wurm, J. Bucher, S. B. Duckworth, M. Rudolph, F. Rominger and A. S. K. Hashmi, *Angew. Chem., Int. Ed.*, 2017, **56**, 3364.



- 12 For recent reviews on ynamide reactivity, see: (a) Y.-C. Hu, Y. Zhao, B. Wan and Q.-A. Chen, *Chem. Soc. Rev.*, 2021, **50**, 2582; (b) C. C. Lynch, A. Sripada and C. Wolf, *Chem. Soc. Rev.*, 2020, **49**, 8543; (c) Y.-B. Chen, P.-C. Qian and L.-W. Ye, *Chem. Soc. Rev.*, 2020, **49**, 889; (d) F.-L. Hong and L.-W. Ye, *Acc. Chem. Res.*, 2020, **53**, 2003; (e) J. Luo, G.-S. Chen, S.-J. Chen, J.-S. Yu, Z.-D. Li and Y.-L. Liu, *ACS Catal.*, 2020, **10**, 13978; (f) B. Zhou, T.-D. Tan, X.-Q. Zhu, M. Shang and L.-W. Ye, *ACS Catal.*, 2019, **9**, 6393; (g) G. Evano, C. Theunissen and M. Lecomte, *Aldrichimica Acta*, 2015, **48**, 59; (h) X.-N. Wang, H.-S. Yeom, L.-C. Fang, S. He, Z.-X. Ma, B. L. Kedrowski and R. P. Hsung, *Acc. Chem. Res.*, 2014, **47**, 560.
- 13 For recent selected examples by our group, see: (a) G.-Y. Zhu, J.-J. Zhou, L.-G. Liu, X. Li, X.-Q. Zhu, X. Lu, J.-M. Zhou and L.-W. Ye, *Angew. Chem., Int. Ed.*, 2022, **61**, e202204603; (b) Z.-S. Wang, L.-J. Zhu, C.-T. Li, B.-Y. Liu, X. Hong and L.-W. Ye, *Angew. Chem., Int. Ed.*, 2022, **61**, e202201436; (c) Y.-Q. Zhang, Y.-B. Chen, J.-R. Liu, S.-Q. Wu, X.-Y. Fan, Z.-X. Zhang, X. Hong and L.-W. Ye, *Nat. Chem.*, 2021, **13**, 1093; (d) P.-F. Chen, B. Zhou, P. Wu, B. Wang and L.-W. Ye, *Angew. Chem., Int. Ed.*, 2021, **60**, 27164; (e) Y.-Q. Zhang, Y.-P. Zhang, Y.-X. Zheng, Z.-Y. Li and L.-W. Ye, *Cell Rep. Phys. Sci.*, 2021, **2**, 100448; (f) Z.-S. Wang, Y.-B. Chen, H.-W. Zhang, Z. Sun, C. Zhu and L.-W. Ye, *J. Am. Chem. Soc.*, 2020, **142**, 3636; (g) X. Liu, Z.-S. Wang, T.-Y. Zhai, C. Luo, Y.-P. Zhang, Y.-B. Chen, C. Deng, R.-S. Liu and L.-W. Ye, *Angew. Chem., Int. Ed.*, 2020, **59**, 17984.
- 14 For recent selected examples, see: (a) G. Shen, Z. Wang, X. Huang, M. Hong, S. Fan and X. Lv, *Org. Lett.*, 2020, **22**, 8860; (b) S. DeBonis, D. A. Skoufias, R.-L. Indorato, F. Liger, B. Marquet, C. Laggner, B. Joseph and F. Kozielski, *J. Med. Chem.*, 2008, **51**, 1115; (c) L. Alain and G. Frederic, EP 197232, 2008; (d) B. Hellrung and H. Balli, *Helv. Chim. Acta*, 1980, **63**, 1284.
- 15 For the structures of $\text{NaBAR}^{\text{F}}_4$ and ynamides **1ag–1ai**, see below.



- 16 (a) S. Liao, X.-L. Sun and Y. Tang, *Acc. Chem. Res.*, 2014, **47**, 2260; (b) L. Wang and Y. Tang, *Tetrahedron*, 2022, **129**, 133121.
- 17 CCDC 2192857 ((+)-**2a**).†

